Contribution from the Institut de Chimie Inorganique, Université de Fribourg, Pérolles, CH-1700-Fribourg, Switzerland, and Laboratoire de Photochimie Générale, UA CNRS 431, ENSCMu, F-68093-Mulhouse, France

Electronic Structure and Interpretation of the EPR Parameters of the $Ru(H_2O)_6^{3+}$ and $Ru(NH_3)_6^{3+}$ Ions

CLAUDE DAUL* and ANNICK GOURSOT

Received December 28, 1984

Multiple scattering Xα MO calculations are reported for hexaaquaruthenium(III) and hexaammineruthenium(III). An analysis of the EPR data with inclusion of spin–orbit coupling and trigonal splitting is proposed. A comparison of the experimental and theoretical splitting parameters yields the relative orientation of the water molecules in the $Ru(H_2O)_6^{3+}$ ion. A good agreement is obtained between the calculated and observed properties.

1. Introduction

Only a rather few aqua ions have been thoroughly characterized within the second and third transition-metal series in sharp contrast to the 3d metals. In particular, a well-defined redox couple has been described only for ruthenium. A few studies concerning the electronic structure of $Ru(H_2O)_6^{3+}$ with its low-spin d^5 configuration have been performed in dilute solutions, including the measurement of the optical spectrum[1,2] and a determination of the magnetic susceptibility from ^1H NMR data.[3] A magnetic moment of 2.02–2.06 μ_B (278–329 K and a spin–orbit coupling constant of 1200 (200) cm^{-1} have been reported.[3] The hyperfine splitting constants of $Ru(H_2O)_6^{3+}$ are reduced by at least a factor of 2 compared with those of $Ru(NH_3)_6^{3+}$.[4] This could be partly explained by a $O_{p\pi}$–$Ru_{d\pi}$ interaction, spreading out the spin density onto the ligands for $Ru(H_2O)_6^{3+}$. Following the isolation of stable crystalline salts of $Ru(H_2O)_6^{3+}$ and the measurement of its EPR spectrum,[4] we have initiated a comprehensive study of $Ru(H_2O)_6^{3+}$ and $Ru(NH_3)_6^{3+}$. The present paper discusses the electronic structure and CT spectra of these ions, based on MS–Xα and extended Hückel (EH) MO calculations. The interpretation of the EPR data, in terms of calculated g and a values, allows us to precisely determine the trigonal field splitting as about 2500 cm^{-1} in the $Ru(H_2O)_6^{3+}$ cation and to propose a particular relative orientation of the water molecules. The free rotation of the ammine molecules in $Ru(NH_3)_6^{3+}$ is suggested by the good agreement between the experimental hyperfine parameters and their calculated values, assuming an octahedral site symmetry.

2. Calculation Parameters

The calculations have been performed without spin orientation with the relativistic Xα method,[5] where the effects of the mass–velocity and Darwin corrections are included self-consistently, while those of the spin–orbit operator are neglected. The spin–orbit effects may then be taken into account after self-consistency, by first-order perturbation theory.

For purposes of the present calculation, NH_3 and H_2O ligands were rotated so that the cations have a D_{3d} symmetry. the Ru–O and Ru–N distances are taken as 2.029[6] and 2.104 Å,[7] respectively. The geometry of the H_2O and NH_3 ligands are assumed to be identical with those of the free molecules,[8,9] namely, the O–H and N–H bond lengths are 0.957 and 1.011 Å, and the HOH and HNH bond angles are 104.5 and 106.7°, respectively. The values of the atomic exchange parameter α are taken from ref 10 for Ru(0.702 53), O (0.744 47), and N (0.751 97) and from ref 11 for H (0.777 25). The weighted average value chosen for interatomic and extramolecular rgions is 0.762 96 for $Ru(H_2O)_6^{3+}$ and 0.768 19 for $Ru(NH_3)_6^{3+}$. Overlapping atomic sphere radii were obtained nonempirically[12] as 88% of the atomic number radii. An externally tangent outer sphere is used, which also serves as a "Watson sphere",[13] on which a negative charge of −3 is distributed. Partial waves up to $l = 4$ are included in the multiple-scattering expansion in the Ru sphere and extramolecular region, up to $l = 1$ in the O and N spheres, and up to $l = 0$ in the H spheres.

3. Xα Electronic Structure and Optical Spectra

The theoretical MO study of $Ru(H_2O)_6^{3+}$ and $Ru(NH_3)_6^{3+}$ must pass over the difficulty of the rigid-space representation of the NH_3 and H_2O groups. For $Ru(H_2O)_6^{3+}$, we can choose T_h or D_{3d} symmetries (Figure 1) or every intermediate structure. In the T_h case, the dσ orbitals (d_{z^2}, $d_{x^2-y^2}$) are degenerate, as are the dπ orbitals ($d_{xy,xz,yz}$), and there is no trigonal field splitting. On the contrary, the D_{3d} arrangement leads to a splitting of the t_{2g} MO (O_h) in a_{1g} and e_g MOs and their energy difference measures the trigonal field splitting δ. If the H_2O planes are allowed to rotate around the Ru–O bonds, it is easily seen from Figure 1 that the D_{3d} symmetry ($|\psi| = 45°$) correspond to a maximum value for δ, which decreases until zero for the T_h arrangement of the atoms ($\psi = 0°$). All intermediate values of δ correspond to a lower symmetry, such as C_3, C_i, or C_s. For $Ru(NH_3)_6^{3+}$, there is no possibility of metal–ligand π bonding, related to a probable free-rotation of the NH_3 groups around the Ru–N bonds. The trigonal field splitting is thus expected to be very weak. In fact, according to the EPR data, the hexaammine complex may be considered as an octahedral case.

For both complexes $Ru(H_2O)_6^{3+}$ and $Ru(NH_3)_6^{3+}$, we have thus chosen to perform our Xα calculations in D_{3d} symmetry, which corresponds to the largest possible value of the trigonal field splitting. This has to be kept in mind for the comparison of our results with the EPR data.

The calculated valence levels and corresponding charge distribution of $Ru(H_2O)_6^{3+}$ and $Ru(NH_3)_6^{3+}$ are presented in Tables I and II.

The unpaired electron of $Ru(H_2O)_6^{3+}$ occupies the σ-antibonding $4a_{1g}$ orbital. The energy gap between $5e_g$ and $4a_{1g}$, which measures the trigonal field splitting, amounts to 4900 cm^{-1}. The metal MOs 5eg, $4a_{1g}$, and $6e_g$ have 70% of their charge localized in the metal sphere, leading to a nonnegligible delocalization of the unpaired electron over the water molecules. On the contrary, the unpaired electron of $Ru(NH_3)_6^{3+}$ is located in the nonbonding $4a_{1g}$ MO, which has a strong metallic character since 86% of its charge is localized in the Ru sphere. For this complex, the trigonal $4a_{1g}$–$5e_g$ splitting is very weak (about 400 cm^{-1}), in relation to the nonbonding character of both $5e_g$ and $4a_{1g}$ MOs. This result is consistent with the largest spin density on the metal for $Ru(NH_3)_6^{3+}$, as suggested by the largest values of its hyperfine tensor components, compared with the values for $Ru(H_2O)_6^{3+}$.

The ligand field spectra of $Ru(H_2O)_6^{3+}$ and $Ru(NH_3)_6^{3+}$ have already been assigned, by application of the ligand field theory.[2,4,14-16] The intense parts of their spectra have been assigned

* To whom correspondence should be addressed at Institut de Chimie Inorganique.

(1) Kallen, T. W.; Earley, J. E. *Inorg. Chem.* **1971**, *10*, 1149.
(2) Harzion, Z.; Navon, G. *Inorg. Chem.* **1980**, *19*, 2236.
(3) Harzion, Z.; Navon, G. *Inorg. Chem.* **1982**, *21*, 2606.
(4) Bernhard, P.; Stebler, A.; Ludi, A., submitted for publication.
(5) Wood, H. J.; Boring, M. *Phys. Rev. B* **1978**, *18*, 2701.
(6) Bernhard, P.; Bürgi, H. B.; Hauser, J.; Lehmann, H.; Ludi, A. *Inorg. Chem.* **1982**, *21*, 3936.
(7) Stynes, H. C.; Ibers, J. A. *Inorg. Chem.* **1971**, *10*, 2304.
(8) Kuchitsu, K.; Bartell, L. S. *J. Chem. Phys.* **1962**, *36*, 2460.
(9) Kuchitsu, K.; Guillory, J. P.; Bartell, L. S. *J. Chem. Phys.* **1968**, *49*, 2488.
(10) Schwarz, K. *Phys. Rev. B* **1972**, *5*, 2466.
(11) Slater, J. C. *Int. J. quantum Chem., Symp.* **1973**, *7*, 533.
(12) Norman, J. G. *Mol. Phys.* **1970**, *31*, 1191.
(13) Watson, R. E. *Phys. Rev.* **1958**, *3*, 1108.
(14) Guenzburger, D.; Garnier, A.; Danon, J. *Inorg. Chim. Acta* **1977**, *21*, 119.
(15) Mc Caffery, A. J.; Rowe, M. D. *J. Chem. Soc., Dalton Trans.* **1973**, 1605.
(16) Navon, G.; Sutin, N. *Inorg. Chem.* **1974**, *13*, 2159.

0020-1669/85/1324-3554$01.50/0

Table I. Ground-State Energy Levels[a] and Charge Distribution of $Ru(H_2O)_6^{3+}$ in D_{3d} Symmetry

		Ru				O		H		
MO	*E*, Ry	s	p	d	f	s	p	s	int	out
$5a_{1g}$	−0.126	2				7		1	49	41
$6e_g$	−0.370			70		6	17	3	3	1
$4a_{1g}$	−0.564			67			24		8	1
$5e_g$	−0.609			71			20		9	
$5e_u$	−0.754				1		78		21	
$4a_{2u}$	−0.768				1	1	75		22	1
$4e_g$	−0.769			18			63	1	18	
$3a_{1g}$	−0.869			25			51		24	
$4e_u$	−0.985		5		1	4	70	13	6	1
$3a_{2u}$	−0.989		5		1	4	69	12	7	2
$2a_{1g}$	−1.085	11				2	64	13	9	1
$3e_g$	−1.113			27		1	56	11	4	1
$1a_{2g}$	−1.183						66	33		1
$1a_{1u}$	−1.199						66	33		1
$3e_u$	−1.209						66	33		1
$2e_g$	−1.225			2			65	32		
$2e_u$	−2.109		1			78		20		1
$2a_{2u}$	−2.109		1			78		20		1
$1e_g$	−2.113		1			78		20		1
$1a_{1g}$	−2.126	1				78		20		1
$1a_{2u}$	−3.745		99						1	
$1e_u$	−3.745		99						1	

[a] The highest occupied level is $4a_{1g}$, which accommodates one electron.

Table II. Ground-State Energy Levels[a] and Charge Distribution of $Ru(NH_3)_6^{3+}$ in D_{3d} Symmetry

		Ru				N		H_1	H_2		
MO	*E*, Ry	s	p	d	f	s	p	s	s	int	out
$5a_{1g}$	−0.106					9				40	51
$6e_g$	−0.143			56		6	26		1	6	5
$4a_{1g}$	−0.500			86			3	2	1	8	
$5e_g$	−0.504			85			2	1	3	9	
$5e_u$	−0.626		6		1	4	63	1	5	17	3
$4a_{2u}$	−0.627		6		1	3	64	4	2	17	3
$3a_{1g}$	−0.771	15					55	2	4	21	3
$4e_g$	−0.808			40		7	35	2	4	11	1
$1a_{2g}$	−0.936						58		39	1	2
$3e_g$	−0.936						58	21	19		2
$4e_u$	−0.959						56	15	23	4	2
$1a_{1u}$	−0.979						54		39	5	2
$3a_{2u}$	−0.985						54	23	14	7	2
$3e_u$	−0.987						54	12	25	7	2
$2e_g$	−1.022			4			50	5	29	10	2
$2a_{1g}$	−1.030			4			50	23	11	11	1
$1e_g$	−1.706			2		69		9	19		1
$1a_{1g}$	−1.736	2				67		10	18	2	1
$1a_{2u}$	−3.571		100								
$1e_u$	−3.571		100								

[a] The highest occupied level is $4a_{1g}$, which accomodates one electron.

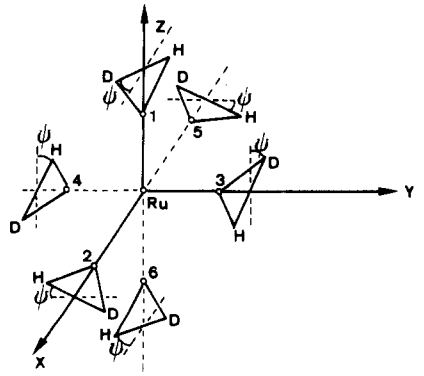

Figure 1. Symmetrical shape of hexaaquaruthenium(III) ($\psi = 0°$, symmetry T_h; $|\psi| = 45°$, symmetry D_{3d}). By drawing the water molecules as hydrogen deuterium oxide, their orientation with respect to the Ru–O bond has been fully specified.

to CT transitions,[2,14,15,17,18] but more precise assignments can be proposed, based on Xα transition states and calculated transition moments from EHMOs.[19] They are reported in Table III for $Ru(H_2O)_6^{3+}$ and Table IV for $Ru(NH_3)_6^{3+}$.

Table III. Xα Calculated LMCT Excitation Energies, Calculated Transition Dipole Moments,[a] and Experimental Peak Positions of $Ru(H_2O)_6^{3+}$ (D_{3d} Symmetry) (cm^{-1})

transitions[b]	calcd energies	calcd transition moments	exptl peak positions[c]
$5e_u \rightarrow 4a_{1g}$ A	26 500	0.06	ligand field spectrum
$4e_g \rightarrow 4a_{1g}$ F	27 200		20–30 000
$3a_{1g} \rightarrow 4a_{1g}$ F	37 500		($\epsilon < 200$)
$5e_u \rightarrow 6e_g$ A	48 100	1.57	45 000
$4e_u \rightarrow 4a_{1g}$ A	51 400	1.98	($\epsilon = 2860$)

[a] For allowed transitions. [b] Key: A, allowed; F, forbidden by the symmetry selection rules. [c] Solution spectrum.[2]

(17) Jørgensen, C. K. "Absorption Spectra and Chemical Bonding in Complexes"; Pergamon Press: Oxford England, 1962.
(18) Ondrechen, M. J.; Ratner, M. A.; Ellis, D. E. *J. Am. Chem. Soc.* **1981**, *103*, 1656.

Table IV. Xα Calculated LMCT Excitation Energies, Calculated Transition Dipole Moments,[a] and Experimental Peak Positions of $Ru(NH_3)_6^{3+}$ (D_{3d} Symmetry) (cm^{-1})

transitions[b]	calcd energies	calcd transition moments	exptl peak positions
$5e_u \rightarrow 4a_{1g}$ A	23 200	0.29	23 000 (ϵ = 0.5)
$3a_{1g} \rightarrow 4a_{1g}$ F	35 900		36 400
$4e_g \rightarrow 4a_{1g}$ F	38 000		(ϵ = 480)
$3e_g \rightarrow 4a_{1g}$ F	55 900		
$5e_u \rightarrow 6e_g$ A	56 100	2.78	50 000
$4e_u \rightarrow 4a_{1g}$ A	58 300	0.93	(ϵ very high)
$3e_u \rightarrow 4a_{1g}$ A	61 000	0.73	

[a] For allowed transitions. [b] Key: A, allowed; F, forbidden by the symmetry selection rules.

(a) $Ru(H_2O)_6^{3+}$. The only intense absorption band in the spectrum of $Ru(H_2O)_6^{3+}$ is located near 45 000 cm^{-1}; the other absorptions at 25 000 and 35 000 cm^{-1} are weak and have been assigned to ligand field transitions.[2,4] The CT transitions reported in Table III refer to calculations performed in D_{3d} symmetry. As will be shown further, the D_{3d} arrangement of the water molecules, which leads to the largest trigonal field splitting δ, does not correspond to the real one. Anticipating the magnetic results, we can say that δ only amounts to 2500 cm^{-1} while the D_{3d} Xα-calculated splitting is 4900 cm^{-1}. All the reported CT transitions involving the $4a_{1g}$ (HOMO) level are thus overestimated by about 2000–2500 cm^{-1}, when compared, with spectra of crystalline salts. Two forbidden transitions $4e_g \rightarrow 4a_{1g}$ and $3a_{1g} \rightarrow 4a_{1g}$ will thus be located near 25 000 and 35 500 cm^{-1}, in the low-intensity part of the spectrum, as is the allowed CT transition $5e_u \rightarrow 4a_{1g}$, which has a very small calculated transition moment (0.06). The intense band of the spectrum is assigned to the allowed $5e_u \rightarrow 6e_g$ and $4e_u \rightarrow 4a_{1g}$ CT transitions, which indeed have large calculated transition moments.

Let us note that a T_h situation (δ = 0) would lead to still lower energies for the LMCT transitions populating the $4a_{1g}$ level. In fact, the absorption bands in the crystal occur at higher energy (1000–1500 cm^{-1}) than the corresponding bands in the solution spectrum (Table III). This shift could be related to changes in the orientation of the water molecules, i.e. to symmetry changes.

(b) $Ru(NH_3)_6^{3+}$. The high-intensity band of the spectrum of $Ru(NH_3)_6^{3+}$ occurs at ν_{max} >50 000 cm^{-1}. In the low-energy region, two bands of moderate intensity at 31 300 and 36 400 cm^{-1} and a shoulder at 47 600 cm^{-1} have been assigned to spin-allowed ligand field transitions,[14,16] A very weak band at 23 000 cm^{-1} is generally assigned to a spin-forbidden ligand field transition.[14,16]

From our calculations (Table IV), and as already suggested previously,[14] the band at 36 400 cm^{-1} is also assigned to parity-forbidden CT transitions, from the ammine $3a_{1g}$, $4e_g$ levels to the incomplete metal t_{2g} level. The very intense absorption rising after 50 000 cm^{-1} is principally assigned to the parity-allowed $5e_u \rightarrow 6e_g$ ($t_{1u} \rightarrow e_g$) and $4e_u \rightarrow 4a_{1g}$ ($t_{2u} \rightarrow t_{2g}$) CT transitions, which have large calculated transition moments. The first allowed transition $5e_u \rightarrow 4a_{1g}$ ($t_{1u} \rightarrow t_{2g}$) is calculated at 23 200 cm^{-1}. There is only a very weak absorption at 23 000 cm^{-1} in the experimental spectrum, which has been assigned to a doublet–quartet d–d transition. However, the presence of a ligand t_{1u} level situated between the metal t_{2g} and the ammine e_g and a_{1g} levels is unquestionable and consistent with the EH results (this work and ref 6) and previous calculations on $Co(NH_3)_6^{3+}$.[20] We are thus led to conclude that the calculated transition dipole moment relative to this transition (1.29) has a strongly overestimated value.

4. Interpretation of the g and a Tensors

(a) $Ru(H_2O)_6^{3+}$. In low-spin d^5 complexes the unpaired electron occupies the t_{2g} orbitals, which are split under the combined effect of noncubic ligand fields and spin–orbit coupling. Analytical expressions for $g_\parallel$, $g_\perp$, $a_\parallel$ and $a_\perp$ are derived by considering spin–orbit coupling, trigonal field splitting, and Zeeman and hyperfine interaction and by using trigonally quantized real d orbitals.

The influence of excited configurations will be neglected on the basis of our MS–Xα results.

Taking the threefold axis as axis of quantization, the three t_{2g} wavefunctions are

$$|e_x\rangle = (2/3)^{1/2}(x^2 - y^2) - (1/3)^{1/2}xz$$
$$|e_y\rangle = (2/3)^{1/2}xy + (1/3)^{1/2}yz \qquad (1)$$
$$|a_1\rangle = z^2$$

with energies 0, 0, and δ, respectively.

The six five-electron states may be taken as

$$|\psi_1\pm\rangle = |a_1^{\pm}e_x^2e_y^2\rangle$$
$$|\psi_2\pm\rangle = \pm 1/2^{1/2}|a_1^2e_x^{\mp}e_y^2\rangle - i/2^{1/2}|a_1^2e_x^2e_y^{\mp}\rangle \qquad (2)$$
$$|\psi_3\pm\rangle = \pm 1/2^{1/2}|a_1^2e_x^{\mp}e_y^2\rangle + i/2^{1/2}|a_1^2e_x^2e_y^{\mp}\rangle$$

The matrix of the trigonal ligand field and the spin–orbit coupling factorizes into two identical 3 × 3 matrices

	$\|\psi_1\pm\rangle$	$\|\psi_2\pm\rangle$	$\|\psi_3\pm\rangle$
$\langle\psi_1\pm\|$	$-\delta$	$-\zeta/2^{1/2}$	0
$\langle\psi_2\pm\|$	$-\zeta/2^{1/2}$	$\zeta/2$	0
$\langle\psi_3\pm\|$	0	0	$-\zeta/2$

where ζ is the spin–orbit coupling constant.

The lowest Kramers doublet must be of the form

$$|+\rangle = a_1|\psi_1+\rangle + a_2|\psi_2+\rangle \qquad |-\rangle = a_1|\psi_1-\rangle + a_2|\psi_2-\rangle \qquad (3)$$

where

$$a_1 = \sin\theta \text{ if } \theta \geq 0$$
$$= \cos\theta \text{ if } \theta < 0$$
$$a_2 = \cos\theta \text{ if } \theta \geq 0$$
$$= -\sin\theta \text{ if } \theta < 0$$
$$\tan 2\theta = (\zeta 2^{1/2}/(\zeta/2) - \delta)$$

To determine the components of the **g** tensor, we must evaluate the matrix elements of $\beta\vec{H}\cdot(2\vec{S} + k\vec{L})$ within these two states and compare them with the corresponding elements of $\beta\vec{H}\cdot\mathbf{g}\cdot\vec{S}$ within states $S = {}^1/_2$, $M_s = \pm{}^1/_2$. We thus obtain

$$g_\parallel = 2a_1^2 - 2(1 + k)a_2^2 \qquad g_\parallel = 2a_1^2 + 2.828ka_1a_2 \qquad (4)$$

where k is the orbital reduction factor describing the reduction of the orbital angular momentum caused by the delocalization of d-electron density onto the ligands. The components of the **a** tensor can be evaluated in a similar way. We determined the matrix elements of

$$P[\vec{L} - K\vec{S} + {}^1/_7\sum_{i=1}^{5}4\vec{S}_i - (\vec{l}_i\vec{s}_i)\vec{l}_i - \vec{l}_i(\vec{l}_i\vec{s}_i)]\vec{I}$$

where P is the usual anisotropic hyperfine parameter and $KP\vec{S}\cdot\vec{I}$ describes the Fermi contact interaction, and compared them with the corresponding elements of $\vec{S}\cdot\mathbf{a}\cdot\vec{I}$. The obtained expressions are

$$a_\parallel = P[0.571a_1^2 - 0.404a_1a_2 - 1.714a_2^2 - K(a_1^2 - a_2^2)]$$
$$a_\perp = P[-0.286a_1^2 + 3.030a_1a_2 - 0.286a_2^2 - Ka_1^2] \qquad (5)$$

The experimental g and a values are[4]

$$|g_\parallel| = 1.489 \qquad |g_\perp| = 2.514$$
$$|a_\parallel| = 22 \times 10^{-4}\ cm^{-1} \qquad |a_\perp| = 10^{-4}\ cm^{-1}$$

From the expressions of (4) and (5) and the experimental values of $g_\parallel$, $g_\perp$, $a_\parallel$, and $a_\perp$, a best fit can be obtained for two distinct

(19) Daul, C.; Schläpfer, C. W., submitted for publication in *Inorg. Chem.*
(20) Goursot, A.; Penigault, E.; Weber, J. *Chem. Phys.* **1979**, *38*, 11.

Table V. MS-Xα Detailed Contributions (Spin-Restricted Calculation) to the Calculated g Factors and Hyperfine Tensors of the $Ru(H_2O)_6^{3+}$ and $Ru(NH_3)_6^{3+}$ Ions (Assumed D_{3d} Symmetry) and Comparison with Experiment

param[a]	$Ru(H_2O)_6^{3+}$ [c]	$Ru(NH_3)_6^{3+}$ [c]
k	0.865	0.959
ζ_{4d}, cm^{-1}	1007	1150
P_0, 10^{-4} cm^{-1}	60.56	54.81
P, 10^{-4} cm^{-1}	45.61	50.49
A_F, 10^{-4} cm^{-1}	-30.39	-31.12
K	0.502	0.616
$g_\parallel$	1.47[b] (1.49)	-1.94 ($\simeq$1.925)
$g_\perp$	2.52[b] (2.51)	
$a_\parallel$	-13.90[b] (22.0)	-47.32 ($\simeq$48.5)
$a_\perp$	-1.47[b] (0.0)	

[a] k is the orbital reduction factor; ζ_{4d} is the spin-orbit parameter of the $4a_{1g}$ MO; $P_0 = g_e g_{Ru} \beta_e \beta_{Ru} \langle r^{-3} \rangle$ for $4a_{1g}$; $P = \rho_M P_0$, where ρ_M is the Xα 4d charge distribution in the metal sphere for $4a_{1g}$; A_F is the Fermi term; $K = -A_F/P$ is the contact parameter. [b] All parameters taken from the D_{3d} calculation, except $\delta = 2500$ cm^{-1}. [c] Experimental values in parentheses from ref 4 for $Ru(H_2O)_6^{3+}$ and from ref 24 for $Ru(NH_3)_6^{3+}$.

sets of solutions (quadratic equations). Solution 1: $\delta/\zeta = 2.5516$, $k = 0.8642$, $P = 80 \times 10^{-4}$ cm^{-1}, $K = 0.6432$. Solution 2: $\delta/\zeta = 0.3473$, $k = 1.1553$, $P = 36.2 \times 10^{-4}$ cm^{-1}, $K = 2.672$. We believe that solution 2 has to be rejected for several reasons: (i) $k > 1$, meaning a delocalization of ligand electrons onto the metal; (ii) such a large value of K (2.672), particularly for a non-heavy-metal atom as Ru; (iii) a theoretical prediction of these parameters based on our MS-Xα calculation in D_{3d} symmetry being much more close to solution 1 than to solution 2 (cf. Table V).

In order to calculate the absolute magnitude of the trigonal splitting δ, the spin-orbit coupling constant ζ should be known. The spin-orbit coupling constant for the free Ru^{3+} ion has been reported to be 1197 cm^{-1}.[21] If this value is multiplied by $k = 0.86$ to account for the delocalization of the 4d electrons onto the ligands, a reasonable estimate of $\zeta = 1000$ cm^{-1} for $Ru(H_2O)_6^{3+}$ is thus obtained. This value is in very good agreement with the MS-Xα calculated one (1007 cm^{-1}) (for details on ζ_{nl} MS-Xα calculations, see ref 22). The trigonal-splitting parameter can then be calculated, and a value of $\delta = 2550$ cm^{-1} is thus obtained. This value is small as compared to the theoretical Xα prediction in D_{3d} symmetry (4900 cm^{-1}). We are thus led to conclude that the trigonal splitting is intermediate between a D_{3d} ($\delta = 4900$ cm^{-1}) and a T_h ($\delta = 0$) value. δ can then be considered as a function of the rotation angle ψ of the H_2O plane around Ru-O bond. This relation can easily be described by using the angular overlap model (AOM), in which only the angular dependence upon the metal-ligand interaction is considered, ligand-ligand interactions being neglected. However, the former interaction is the dominant one.

When the trigonal symmetry is imposed on the hexaaqua ion, only 2 degrees of freedom remain from the set of six rotations about the metal-oxygen bonds. This can be visualized by examination of Figure 1. The water molecules with molecular planes coinciding with xz (ligand no. 1) and with yz (ligand no. 4) are used to generate the positions of the other water molecules by the operation C_3 about the (1,1,1) direction. The 2 degrees of freedom are the rotation angles ψ_1 between the molecular plane of water no. 1 and xz, and the rotation angle ψ_2 between the molecular plane of water no. 4 and yz. Moreover, if $\psi_1 = \psi_2$ modulo π, the hexaaqua ion possesses a center of inversion. When $\psi_1 = \psi_2 = 0$, the symmetry is T_h and δ is equal to zero by symmetry. When $\psi_1 = -\psi_2 = 45°$, the symmetry is D_{3d} and δ is maximum. Application of the angular overlap model (AOM)[23] to this problem yields the following expression for δ:

$$\delta = 3e_\pi \cos(\psi_1 + \psi_2) \sin(\psi_1 - \psi_2) \quad (6)$$

(21) Blume, M.; Freeman, A. J.; Watson, R. E. *Phys. Rev.* **1964**, *134*, A320.
(22) Goursot, A.; Chermette, H. *Chem. Phys.* **1982**, *69*, 329.
(23) Larsen, E.; La Mar, G. N. *J. Chem. Educ.* **1974**, *51*, 633.

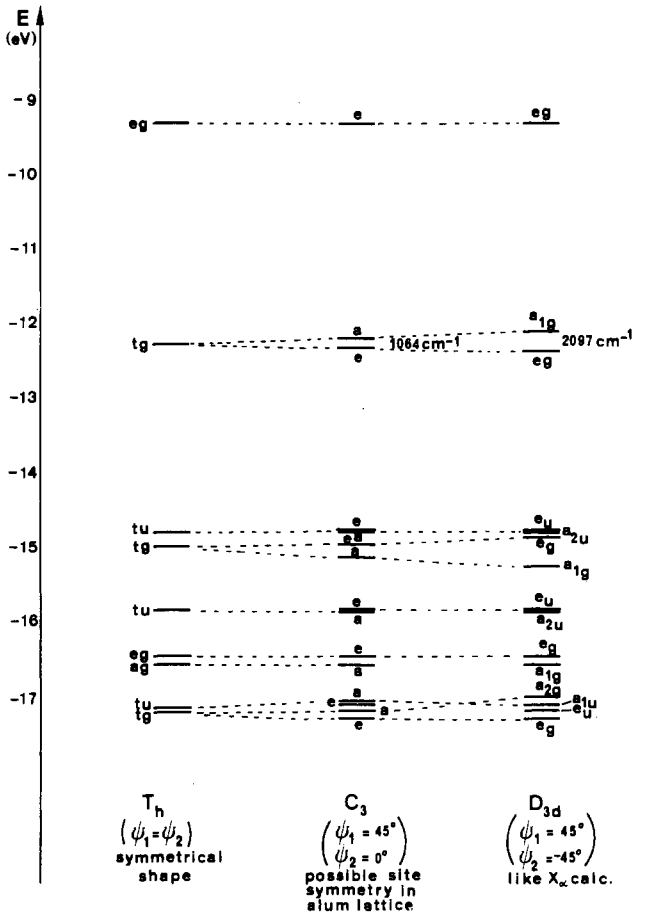

Figure 2. Extended Hückel MO calculation of $Ru(H_2O)_6^{3+}$ for zero, intermediate, and high trigonal splitting.

where e_π is the AOM parameter, which can be determined from our D_{3d} MS-Xα calculation, yielding $e_\pi = 1633$ cm^{-1}. From the EPR data, we have δ(obsd) = 2550 cm^{-1} giving

$$\cos(\psi_1 + \psi_2) \sin(\psi_1 - \psi_2) \simeq 1/2$$

After some goniometric manipulation we obtain

$$\sin 2\psi_1 - \sin 2\psi_2 \simeq 1 \quad (7)$$

There are obviously an infinity of solutions to this equation, but one typical solution is $\psi_1 = 45°$ and $\psi_2 = 0°$.

In order to illustrate this dependancy of the size of the trigonal splitting upon the relative orientations of the water molecules, we have carried out an extended Hückel MO calculation[27] of $Ru(H_2O)_6^{3+}$ (cf. Figure 2), corresponding to three molecular shapes with different trigonal splittings: (i) the zero trigonal field case ($\psi_1 = \psi_2$) with T_h symmetry, (ii) the case of intermediate trigonal splitting ($\psi_1 = 45°$, $\psi_2 = 0°$) corresponding to a probable site symmetry of $Ru(H_2O)_6^{3+}$ in the alum lattice with C_3 symmetry, and (iii) the case of maximal trigonal splitting ($\psi_1 = 45°$, $\psi_2 = -45°$) with D_{3d} symmetry as chosen for our MS-Xα MO calculation (cf. previous section). From inspection of Figure 2 it is seen that only the t_{2g} orbitals of the T_h shape are affected by the relative orientation of the water molecules. This behavior is in agreement with the proposed mechanism of an interaction between the metal t_{2g} orbitals and the π orbitals of water. Even though the absolute size of this interaction is underestimated (Δ_{max}(EHMO) = 2100 cm^{-1}; Δ_{max}(MS-Xα) = 4900 cm^{-1}) by the EHMO semiempirical calculations, the relative trend of the trigonal splitting is clearly shown.

A definitive answer to this question could only be given by an analysis of the neutron diffraction of this compound in order to obtain the location of the H atoms.

(b) $Ru(NH_3)_6^{3+}$. This complex may be considered as a t_{2g}^5 ion in a strong octahedral crystal field since the components of its a tensor are quite similar.[24,25] In fact, the host lattice Co(N-

$H_3)_6Cl_3$ contains three pairs of magnetically inequivalent Ru-$(NH_3)_6^{3+}$ ions. The presence of these three different sites involves thus some uncertainty as to the g and a values. However the traces of g and a are very close for sites I and II ($|\bar{g}| = 1.93$, $|\bar{a}| = 48.3$ for site I and $|\bar{g}| = 1.92$, $|\bar{a}| = 48.7$ for site II) while they are smaller for site III ($|\bar{g}| = 1.88$, $|\bar{a}| = 46.7$). However, these experimental data indicate that the trigonal distortion is very small, at least for sites I and II. This result was already inferred from the MS-Xα calculation, which yields a δ_{max} of 400 cm^{-1} in D_{3d} symmetry.

In the isotropic case ($\delta = 0$), the expressions for g and a become, to first order

$$g = -(2 + 4k)/3 \quad (8)$$

$$a = -2P(^4/_7 - K/6) \quad (9)$$

The calculated g and a values are presented in Table V, together with values of the parameters used for their evaluation. Details concerning the evaluation of k, P, K and ζ_{4d} from Xα calculations may be obtained from ref 23 and 26. For both complexes, P has been evaluated for $4a_{1g}$ through a non-spin-polarized calculation.

Examination of Table V reveals a good agreement between the theoretical g and a values of $Ru(NH_3)_6^{3+}$ and those determined experimentally. The agreement is not so satisfactory for the $a_\parallel$ and $a_\perp$ values of $Ru(H_2O)_6^{3+}$. This discrepancy is probably generated by the use of parameters calculated in the D_{3d} case, with the exception of δ taken as 2500 cm^{-1}, which could differ in a lower symmetry, particularly P and thus K.

As expected from a comparison of the experimental a values of both ions, the orbital reduction factor k and the anisotropic hyperfine parameter P are significantly reduced for the hexaaqua complex, revealing a greater covalency between the metal and the oxygen ligands. Covalency is still more effective than it is apparent through the P values, since P_0 for $Ru(H_2O)_6^{3+}$ is stronger than for the hexaammine ion. This increase is due to the well-known trend of antibonding orbitals to place more charge near the metal nucleus, which leads to larger values of $\langle r^{-3} \rangle$ (let us recall that $4a_{1g}$ is antibonding in $Ru(H_2O)_6^{3+}$ and nonbonding in Ru-$(NH_3)_6^{3+}$).

Core polarization contributes significantly to the hyperfine splitting for both complexes. However, its efficiency is reinforced in the case of $Ru(H_2O)_6^{3+}$ because of the strong values of its coefficients in the expressions in (5). Indeed, K is multiplied by $a_1^2 - a_2^2$ (0.81) for $a_\parallel$ and a_1^2 (0.91) for $a_\perp$ in the case of Ru-$(H_2O)_6^{3+}$, while it contributes to the hyperfine tensor of Ru-$(NH_3)_6^{3+}$ by a factor of $^1/_3$ (expression 9).

5. Conclusion

The aim of this work was to provide a consistent analysis of the electronic and magnetic properties of two d^5 Ru^{3+} complexes, namely $Ru(H_2O)_6^{3+}$ and $Ru(NH_3)_6^{3+}$. The conjoined use of different theoretical approaches (MS-Xα and ligand field methods and the angular overlap model) has allowed us to precisely determine the most important features of their optical and EPR spectra. The magnetic properties of $Ru(NH_3)_6^{3+}$ are described through a strong field octahedral model, with parameters derived from MS-Xα calculations. In contrast, the EPR single-crystal measurements of $Ru(H_2O)_6^{3+}$ are interpreted by considering a trigonal field splitting, which is evaluated at 2500 cm^{-1}. The relative orientation of the water molecules in the crystal is thus derived from a comparison of experimental and theoretical results.

Acknowledgment. Part of the calculations have been performed at the Centre de Calcul CNRS of Strasbourg-Cronenbourg, France.

Registry No. $Ru(H_2O)_6^{3+}$, 30251-72-0; $Ru(NH_3)_6^{3+}$, 18943-33-4.

(24) Griffiths, J. H. E.; Owen, J.; Ward, I. M. *Proc. R. Soc. London, A* **1953**, *A219*, 526.
(25) Griffiths, J. H. E.; Owen, J. *Proc. Phys. Soc., London, Sect. A* **1952**, *65*, 951.
(26) Goursot, A.; Chermette, H. *Inorg. Chem.* **1984**, *23*, 305.
(27) Performed with the same geometry as for the MS-Xα calculation. Single-ζ ligand—a double-ζ metal—STO's were used[23]. Standard VSIE's for neutral ligand atoms were taken, and for Ru, $H_{dd} = -12.7$ eV, $H_{ss} = -9.6$ eV, and $H_{p+} = -6.2$ eV.

Contribution from the Department of Chemistry, Clemson University, Clemson, South Carolina 29631

Photoracemization/Substitution of Optically Active Rhodium(III) Complexes, *cis*-L-$Rh(en)_2(OH)X^{n+}$

LIANGSHIU LEE, STEPHEN F. CLARK, and JOHN D. PETERSEN*

Received July 12, 1984

The photochemistry of *cis*-L-$Rh(en)_2(H_2O)(OH)^{2+}$ and *cis*-L-$Rh(en)_2(OH)_2^+$ in aqueous solution is reported. Irradiation at 313 nm results in a photoracemization quantum yield of 0.05 ± 0.01 and 0.008 ± 0.002 mol/einstein, respectively. The results of this work and previous studies on the photochemistry of *cis*- and *trans*-$Rh(en)_2(OH)X^{n+}$ (X = OH, H_2O) and *cis*- and *trans*-$Rh(en)_2(H_2O)_2^{3+}$ are consistent with a photochemical mechanism involving excitation, ligand labilization, rearrangement of an excited-state, five-coordinate fragment, relaxation, and solvent addition. Ratios of the photochemical quantum yields for cis-L to cis-*rac* and cis to trans conversions agree with the conclusion that $Rh(en)_2(OH)^{2+*}$ is the species undergoing rearrangement in both the dihydroxo and aquo hydroxo systems.

Introduction

The ligand field photolysis of d^6 rhodium(III) amine complexes has been extensively studied over the past decade.[1] This activity is due, in part, to the substitutional inertness and stereoretention of the thermal reactions[2] and the lack of secondary photolysis processes. However, the photoaquation of *cis*-tetraamine-rhodium(III) complexes does lead, in some cases, to trans-disubstituted products.[3-5] For example, the ligand field photolysis of *trans*- and *cis*-dihalobis(ethylenediamine)rhodium(III) complexes results in photoaquation of halo ligand in conjunction with stereoretention for the trans isomer and geometric isomerization for the cis isomer.[3]

Vanquickenborne and Ceulemans[6] have used an "additive point ligand model" to explain the stereochemical changes cited above.

(1) Ford, P. C.; Wink, D.; Dibenedetto, *J. Prog. Inorg. Chem.* **1983**, *30*, 213.
(2) Basolo, F.; Pearson, R. G. "Mechanisms of Inorganic Reactions"; Wiley: New York, 1967; Chapters 3 and 4.
(3) Part 1: Jakse, F. P.; Petersen, J. D. *Inorg. Chem.* **1979**, *18*, 1818. Part 2: Clark, S. F.; Petersen, J. D. *Inorg. Chem.* **1979**, *18*, 3394. Part 3: Clark, S. F.; Petersen, J. D. *Inorg. Chem.* **1980**, *19*, 2917.
(4) Muir, M. M.; Huang, W.-L. *Inorg. Chem.* **1973**, *12*, 1831.
(5) Strauss, D.; Ford, P. C. *J. Chem. Soc., Chem. Commun.* **1977**, 194.
(6) Vanquickenborne, L. G.; Ceulemans, A. *Inorg. Chem.* **1978**, *17*, 2730.

0020-1669/85/1324-3558$01.50/0